Nov 8th, 12:00 AM

Nonlinear Analysis of Steel Space Trusses

Shien T. Wang

George E. Blandford

Christopher D. Hill

Ninth International Specialty Conference on Cold-Formed Steel Structures
St. Louis, Missouri, U.S.A., November 8-9, 1988

NONLINEAR ANALYSIS OF STEEL SPACE TRUSSES

By

Shien T. Wang[1], George E. Blandford[2] and Christopher D. Hill[3]

ABSTRACT

An investigation of the behavior of thin-walled steel space truss structures under the interaction of local, member, and overall buckling is described. Nonlinearities due to member buckling or tensile yielding and local buckling of component plates of the member are accounted for in the analysis. First-order geometric effects are included using a geometric stiffness matrix. Second-order effects are included through an updated Lagrangian formulation. An incremental/iterative solution strategy utilizing modified Newton-Raphson iterations with a constant arc-length constraint is presented. The method developed traces the sequence of local buckling and member buckling until eventual failure of the entire structure.

INTRODUCTION

Space truss systems have been found to be very effective in structures requiring large, unobstructed areas of useful space. Unfortunate failures of truss systems in the past (Lev Zetlin and Associates, 1978), however, have clearly shown that a wide variety of factors affect the stability and carrying capacity of a truss system. Space truss stability has been the focus of much research work in the past (Task Committee on Latticed Structures, 1976). Most research work has been in two general areas: snap-through behavior of curved, dome-type structure and the collapse of layered grid due to progressive failure of the member.

Snap-through behavior has typically been modeled by considering member properties to be elastic (Chu and Rampetsreiter, 1972; Rosen and Schmidt, 1979). Other researchers (Jagannathan, Epstein, and Christiano, 1975; Papadrakakis, 1983) incorporated material nonlinearities. Layered grids were analyzed under the influence of member failures (Lev Zetlin and Associates, 1978; Prickett and Mueller, 1983). Only recently, the effects

---

[1]Professor, Department of Civil Engineering, University of Kentucky, Lexington, KY 40506-0046

[2]Associate Professor, Department of Civil Engineering, University of Kentucky, Lexington, KY 40506-0046

[3]Structural Engineer, Department of Transportaion, State of Kentucky, Frankfort, KY

of local buckling coupled with column buckling on the stability and post buckling behavior of space trusses were considered by Bevins (1985); and Wang and Bevins (1987). An incremental/iterative solution strategy with a constant arc-length constraint was developed by Blandford, Wang and Hill (1988) for the analysis of elastic space trusses with large displacements.

The behavior of space truss systems can only be adequately evaluated with all factors, i.e. first and second-order geometric nonlinearity, member failure (yielding or buckling) and local buckling of the component plates of the truss member, are consideed simultaneously. The purpose of this paper is to present an investigation to account for these factors together utilizing the incremental/iterative solution procedure with a constant arc-length constraint. The method developed traces the sequence of local buckling and member buckling until eventual failure of the entire structure. Interesting results have been obtained to shed light on the effects of such factors on the carrying capacity of the space truss structures.

ELEMENT BEHAVIOR

Accurate representation of space truss behavior necessitates using accurate models for element behavior. The element modes of behavior to be modeled include tension yield, elastic member post-buckling response and post-local-buckling of the the member component plates. Each of these topics are discussed in the following paragraphs.

Tension yield and post-yield behavior is represented using the Ramberg-Osgood type stress-strain equation developed by Richard and Blacklock (1969) which is expressed as

$$\sigma(\epsilon) = \frac{E\epsilon}{\left\{ 1 + \left[\frac{E\epsilon}{\left[1 - \frac{E_p}{E} \right] \sigma_k + E_p \epsilon} \right]^n \right\}^{\frac{1}{n}}} \qquad (1)$$

where E is the initial elastic modulus; E_p is the plastic modulus; σ_k is the stress level at which plastic region begins; n is a shape parameter ($n = \ln(2)/\ln(\sigma_k/\sigma_o)$); ϵ is the axial strain and σ_o is the stress level at the end of the elastic region. Equation 1 is shown schematically in Fig. 1.

Elements subjected to compressive loads may at some point begin to fail in any one of three different column buckling modes. Members that are relatively short will typically fail first in torsional or torsional-flexural buckling. Members of intermediate length will commonly fail by torsional-flexural or weak axis Euler buckling and long members will fail by weak axis Euler buckling. Since the failure mode of any particular member is unknown prior to the analysis, the inclusion of member failure requires calculating all three buckling loads for the appropriate cross section, i.e. nonsymmetric, singly symmetric or doubly symmetric which are provided in Timoshenko and Gere (1961).

Elastic pre- and post-buckling behavior is modeled using the stress-strain relationship of Eq. 1. The smallest of the three buckling stresses for the appropriate cross section is used as σ_k in Eq. 1 to model compression behavior up to buckling and E_p is the post-buckling tangent modulus.

Compression members consisting of plate elements with large width-to-thickness ratios, as is typically the case for cold-formed sections, often experience local buckling of the member component plates. Post-local-buckling strength is modeled using the effective width concept (Winter, 1968). As local buckling of the member plates develop, the stress distribution across the width of the locally buckled plate becomes non-uniform. The effective width is the plate width on which an equivalent uniform stress acts to approximate the original non-uniform stress distribution. The effective width equation is expressed as (Wang, Errera and Winter, 1975)

$$\frac{b_e}{t} = 0.95 \sqrt{\frac{kE}{\sigma_{max}}} \left[1 - 0.95\, \xi\, \frac{t}{w} \sqrt{\frac{kE}{\sigma_{max}}} \right] \qquad (2)$$

for

$$\frac{w}{t} \geq 0.64 \sqrt{\frac{kE}{\sigma_{max}}} \qquad (3)$$

in which w is the width and b_e is the effective width of the compression plate element; t is the plate thickness; σ_{max} is the maximum edge stress; stress; k is a coefficient determined by boundary conditions and aspect ratio for the compression plate element; E is the elastic modulus; and ξ is a modification factor based on experimental evidence and engineering judgement to incorporate local imperfections into the equation. For values of w/t smaller than $0.64\ kE/\sigma_{max}$, $b_e = w$. Equation 2 has been shown through experimental verification to be applicable to both stiffened and unstiffened plate elements if k is appropriately adjusted. For uniformly compressed sections, k varies from 4.00 to 6.97 for stiffened plate elements and from 0.425 to 1.28 for unstiffened plate elements. For design considerations, ξ may be considered equal to 0.22 and k may be taken to be 0.50 and 4.0 for unstiffened and stiffened plate elements, respectively.

The stress which will initiate local buckling, σ_{lb}, may be derived from Eq. 3 by replacing σ_{max} with σ_{lb} and solving for σ_{lb}. The local buckling stress can therefore be expressed as

$$\sigma_{lb} = 0.41 \frac{kE}{\left[\frac{w}{t}\right]^2} \qquad (4)$$

Axial stress in excess of σ_{lb} as defined by Eq. 4 initiates the calculation of effective widths for each of the component plates of the member which are then used to modify the member cross-sectional properties. Effective cross-section properties are used to evaluate buckling loads for

the locally buckled sections and an effective area is used in calculating the element stiffness coefficients discussed in the next section.

FINITE ELEMENT FORMULATION

The stiffness equations used to represent the behavior of a typical space truss element are generated using a linear variation of the translational displacements (see Fig. 2), i.e.

$$\{\Delta^e\} = [N]\{p'\} \tag{5}$$

where $\{\Delta^e\}$ is the local element displacement vector $\lfloor u\ v\ w \rfloor^T$; $\{p'\}$ is the local element nodal displacement vector $\lfloor u'_1\ v'_1\ w'_1\ u'_2\ v'_2\ w'_2 \rfloor^T$; [N] is a matrix of linear shape functions; { } signifies column vector; ⌊ ⌋ signifies row vector; and [ ] represents matrix.

A nonlinear, large-displacement analysis of space trusses is achieved using an elastic stiffness matrix and a geometric stiffness matrix representing the linear and nonlinear portions of the structure force-displacement relationship, respectively. The geometric stiffness matrix incorporates the secondary shear forces induced at the element nodes as a result of the combination of axial force and large relative nodal displacements, referred to as the P-delta effect. Elastic and geometric stiffness matrices are generated using the strain-displacement equation

$$\epsilon_x = \frac{du}{dx} + \frac{1}{2}\left[\frac{du}{dx}\right]^2 + \frac{1}{2}\left[\frac{dv}{dx}\right]^2 + \frac{1}{2}\left[\frac{dw}{dx}\right]^2 \tag{6}$$

Many researchers have neglected the axial displacement gradient in Eq. 6 assuming it to be insignificant when strain is small. This assumption is valid only if rotations also happen to be small. Omitting the axial gradient in Eq. 6 produces strain in the element under a rigid body rotation (Jagannathan, Epstein and Christiano, 1975). Therefore, for structural elements undergoing large rotations, as may be expected in evaluating limit loads, all terms in Eq. 6 should be retained.

The element elastic stiffness matrix, $[k'_E]$, and the element geometric stiffness matrix, $[k'_G]$, can be obtained using Eq. 6 and the first theorem of Castigliano to give

$$\{F'\} = \left[\,[k'_E] + [k'_G]\,\right]\{p'\} \tag{7}$$

where $\{F'\}$ is the element force vector,

$$[k'_E] = \frac{E_T A}{\ell}\left[\begin{array}{c|c} I_1 & -I_1 \\ \hline -I_1 & I_1 \end{array}\right], \quad [k'_G] = \frac{F}{\ell}\left[\begin{array}{c|c} I & -I \\ \hline -I & I \end{array}\right],$$

I_1 is a 3x3 matrix in which all coefficients are zero except the 1,1 coefficient which equals 1; I is the 3x3 identity matrix; E_T is the

tangent elastic modulus ($E_T = d\sigma/d\epsilon$); A is the effective cross section area; ℓ is the element length; and F is the element axial force. In arriving at Eq. 7, the quartic inner products of the displacement gradients have been neglected.

Using standard coordinate transformation procedures for space trusses (e.g. Gere and Weaver, 1980) on Eq. 7 leads to

$$\{F^e\} = [k^e]\ \{p^e\} \tag{8}$$

where $\{F^e\}$ is the global element force vector; $[k^e] = [k_E^e] + [k_G^e]$ is the global coordinate element stiffness matrix; and $\{p^e\}$ is the global element displacement vector. Assembling Eq. 8 over all the elements using direct stiffness assembly leads to the structure stiffness equations which are expressed as

$$\{P\} = [K]\{p\} \tag{9}$$

where $\{P\} = \Sigma\ \{F^e\}$ is the structure concentrated force vector; $\{p\}$ is the structure displacement vector; and $[K] = \Sigma\ [k^e]$, consistent with direct stiffness assembly, is the structure stiffness matrix.

Development of the nonlinear element stiffness equation (Eq. 7) is based on a large-displacement formulation. Neglecting the higher order terms (i.e. the quartic products of the displacement gradients) resulted in a first-order nonlinear system of element stiffness equations. Inclusion of the higher order terms results in an additional stiffness matrix, $[k_L']$, providing a small-strain (large strains can only be accurately modeled if the effect of distorting the member area is included; Bathe, 1982), large-rotation, large-displacement system of second-order element stiffness equations (i.e. $\{F'\} = ([k_E'] + [k_G'] + [k_L'])\ \{p'\}$) in the context of a total Lagrangian (T.L.) formulation. In lieu of a T.L. formulation, a second-order analysis can be developed using an updated Lagrangian (U.L.) formulation.

An U.L. formulation consists of updating the reference coordinate system in which the small-strain, small-rotation, large-displacement first-order stiffness equations, Eq. 7, are evaluated from one iteration to the next in the incremental solution algorithm. While coordinate updating is usually done between load steps in an incremental solution to account for the higher order terms that have been neglected in the stiffness matrix, i.e. $[k_L']$, inclusion of the axial displacement gradient in the current analysis requires a coordinate transformation for each iteration. Provided each iterative step is small enough to prohibit significant second-order effects from being generated in the individual truss members, Eq. 7 remains valid over the entire step length and is therefore an appropriate approximation to the equilibrium equations for the structural configuration at the beginning of the iteration. The U.L. scheme is well suited to the modified Newton-Raphson iterative strategy since the coordinate transformation only influences the balanced force calculations within a load step. Therefore no additional evaluations of

the structure stiffness matrices, $[K_E]$ and $[K_G]$, need to be performed within a load step.

Updating the structure coordinates at the end of each iteration causes changes in the "stiffness" associated with the structure free degrees of freedom. In order to maintain consistency in the analysis, the element forces developed by application of Eq. 7 over the previous iteration must be transformed to coincide with the "stiffness" of the updated coordinate system for the structure. Transformation of the local coordinate element forces from the coordinate system in load step m+1 iteration i to that of load step m+1 iteration i+1 requires a reference frame common to iterations i and i+1. The global coordinate system serves as the common reference frame to achieve the transformation. Element force transformations from iteration i to i+1 are expressed in the following two-step process. Step one involves calculating the global coordinate element forces, i.e.

$$ {}^{m+1}\{F^e\}^{(i)} = {}^{m+1}[R]^{(i)} \; {}^{m+1}\{F'\}^{(i)} \qquad (10) $$

where ${}^{m+1}\{F'\}^{(i)}$ is the local coordinate element force vector at the end of iteration i in load step m+1; ${}^{m+1}[R]^{(i)}$ is the element rotation matrix corresponding to the coordinate system of iteration i in load step m+1; and ${}^{m+1}\{F^e\}^{(i)}$ is the global coordinate element force vector at the end of iteration i in load step m+1. Step two involves calculating the local coordinate element forces in terms of the geometry at iteration i+1 in load step m+1, i.e.

$$ {}^{m+1}\{F'\}^{(i+1)} = \left[{}^{m+1}[R]^{(i+1)}\right]^T {}^{m+1}\{F^e\}^{(i)} \qquad (11) $$

where ${}^{m+1}\{F^e\}^{(i)}$ is defined by Eq. 10; ${}^{m+1}[R]^{(i+1)}$ is the element rotation matrix corresponding to the updated coordinate system for iteration i+1 in load step m+1; and ${}^{m+1}\{F'\}^{(i+1)}$ is the transformed local coordinate element force vector for use in iteration i+1 of load step m+1.

NONLINEAR ANALYSIS

A nonlinear analysis which includes only the elastic and geometric stiffness matrices is referred to as a first-order nonlinear analysis. A second-order analysis is obtained using an updated Lagrangian (U.L.) formulation on the first-order nonlinear stiffness equations. An U.L. formulation consists of updating the reference coordinate system for the small-strain, small-rotation, large-displacement first-order stiffness equations, i.e.

$$ ({}^m[K_E] + {}^m[K_G]) \; \{\delta p\}^{(i)} = {}^{m+1}\lambda^{(i)} \; \{P\} - {}^{m+1}\{F\}^{(i-1)} \qquad (12) $$

where

$\{\delta p\}$ - iterative displacement vector,

$\{P\}$ - reference external load vector,

$\{F\}$ - equilibrated internal force vector,

λ - load multiplier,

and the pre-superscript signifies the load level with m+1 being the current load step whereas the supercript in parentheses signifies the iteration number. Accumulated incremental displacement and load vectors along with the load multiplier λ are generated using the constant spherical arc-length formulation of Crisfield (1983) with a modified Newton-Raphson iteration strategy. Coordinate updating is usually done between load steps in an incremental solution to account for the neglected higher order terms. However, performing a coordinate transformation for each iteration results in a better approximation. This is particularly important in the present formulation since the axial strain gradient has been included in the geometric stiffness matrix. The U.L. scheme is well suited to the modified Newton-Raphson iterative strategy since the coordinate transformation only influences the balanced force calculations within a load step. Therefore, no additional evaluations of the structure stiffness matrices, $[K_E]$ and $[K_G]$, need to be performed within a load step.

Convergence to an equilibrium condition in Eq. (12) is evaluated in terms of the internal energy (Bathe, 1982), i.e.

$$\frac{\lfloor \delta p \rfloor^{(i)} \left({}^{m+1}\lambda^{(i)} \{P\} - {}^{m+1}\{F\}^{(i)} \right)}{\lfloor \delta p \rfloor^{(1)} \left({}^{m+1}\lambda^{(1)} \{P\} - {}^{m}\{F\} \right)} < \epsilon_E \qquad (13)$$

where ϵ_E is the energy error tolerance ($1 \times 10^{-10} \leq \epsilon_E \leq 1 \times 10^{-6}$).

NUMERICAL RESULTS

Truss system performance is investigated for four space trusses labeled T1 - T4. The various material and geometric nonlinearities discussed in the development sections of the paper are considered. Member types used for trusses T1 - T4 are presented in Table 1 with the corresponding member properties given in Table 2. Based on the solution procedures outlined, a finite element program STAP (Space Truss Analysis Program) has been developed and is used in this study.

The toggle truss of Fig. 3 (T1) has been analyzed by many researchers. Recent work by Kondoh and Atluri (1985) is compatible with the current analysis and will be used for comparison. For purposes of comparison, elastic post-buckling is modeled by setting E_p in Eq. 1 equal to the elastic post-buckling stiffness coefficient derived by Kondoh and Atluri. Based on their derivation $E_p = \pi^2 EI/(2\ell^3)$ for a member buckling elastically. As presented in Fig. 4, the load/deflection response of truss T1 with both members buckling elastically shows excellent agreement with the results of Kondoh and Atluri (1985). Since truss T1 has no internal redundancy, buckling of the truss members leads to immediate failure of the truss. However, the results presented in Fig. 4 show the capability of the nonlinear solution strategy to trace structural response beyond limit points associated with member failure and to remain stable while tracing post-critical member behavior. Additionally, Eq. 1 is shown

to be quite adequate in modeling elastic post-buckling behavior. Results for truss T1 represent "snap-through" behavior. Figure 4 also shows the elastic load/deflection path for truss T1 as determined by STAP. Comparison with the results of Kondoh and Atluri indicates a discrepancy of approximately 1.2 percent at the limit point. The discrepancy is attributable to the finite element approximation made in the current research as opposed to the analytical formulation of Kondoh and Atluri. While it is undesirable to perform the analysis in many very small increments, it is important to note that results have been obtained indicating the current analysis will converge to the analytical results of Kondoh and Atluri when small increments are used. Therefore, any degree of accuracy desired can be obtained in the analysis at the expense of additional computer time.

Analysis of the Thompson strut (T2) shown in Fig. 5 demonstrates the importance of considering local buckling in truss analysis. Neglecting the nonlinearity associated with local buckling can result in erroneous prediction of the space truss systems response to loading. Figure 6 shows a comparison between the linear elastic, geometric nonlinear and geometric nonlinear with local buckling responses of truss T2. The results are in excellent agreement with that obtained by Wang and Bevins (1987). Local buckling results in a reduction in the truss limit load from 729 kips to 510 kips as shown in Fig. 6. This is a reduction of approximately 30 percent. The necessity to incorporate local buckling effects in truss analyses is highlighted by such a substantial reduction in the load carrying capacity.

Results obtained for the tower truss (T3) shown in Fig. 7 further illustrates the significant influence of local buckling on space truss load carrying capacity. Local buckling influences can be seen in Fig. 8. Clearly the reduction in the truss stiffness associated with local buckling is the dominant factor in the response of truss T3 provided no member failures occur. While the geometric softening experienced by the truss is almost undetectable, local buckling begins to soften the truss at small loads and substantially reduces the load carrying capacity of the truss. (However, with the cross section properties used for this illustrative example, collapse of the truss occurs at a load level far below the region in which local buckling effects begin to become significant.) The progressive failure of truss T3 when member failures (i.e. member buckling with $E_p = 0$) are considered is shown in Fig. 9 illustrating the nature of a truss systems response to loading as load redistribution occurs. As reflected in Fig. 9, members 18, 19, 20, 21, 26 and 29 fail nearly simultaneously causing a change in the response of the truss. Redistribution of the applied load is reflected by a change of course in the load deflection path. Internal redundancy enables the truss to remain stable under increasing load as the structure deforms along the altered response path. Loading continues until the remaining internal redundancy is eliminated by the failure of members 2 and 3 resulting in failure of the truss at an applied load of 2.1 kips.

The 200 member, 61 node layered grid truss (T4) shown in Fig. 10 is representative of a typical truss system encountered in practice. Progressive member failure in truss systems of this kind is a topic of much concern. An elastic analysis of truss T4 with elastic member buckling is

shown in Fig. 11. Again the original load redistribution that occurs as a result of member failures causes a change in the response of the truss. As expected, failure of members at symmetrical locations at the center of the truss, as shown in Fig. 10, occurs first. Failure of members 25, 30, 31 and 36 at an applied load of 13.14 kips redistributes any additional applied load to the adjacent members in the truss. At an applied load of 13.71 kips, members 14, 29, 32, and 47 are buckled. When members 3, 28, 33 and 58 fail, the truss is unable to accept any additional load. STAP results show failure of the truss occuring at an applied load of 16.58 kips.

CONCLUSIONS

A significant result of the research is that an accurate analysis procedure to access the behavior of truss systems in their failure modes has been developed. An accurate estimate for the limit load of a truss can be generated when nonlinear material and geometric nonlinear responses are included in the analysis. This will also include localized effects such as local buckling and column buckling.

It has been found that local buckling effects reduce the limit load of a truss and the severity of this reduction depends upon the width-to-thickness ratio of the component plates. When considering the effects of member buckling or yielding, the reduction in load carrying capacity of the truss is substantial. Unless the truss is highly redundant, the limit load of the truss is not much larger than the load at which the first member failed. Therefore, the geometry of the truss is an important factor to determine its carrying capacity. Consideration of this reserved strength can be important in quantifying the safety of truss systems, when subjected to overload conditions. Redundancy can provide additional insight into the mechanisms by which truss strength and safety can most effectively be increased. Design modifications such as geometry changes, cross section types and member dimensions can be investigated to evaluate alternative designs.

ACKNOWLEDGEMENT

The research presented in this paper was supported by the National Science Foundation through the EPSCoR program (Computational Science Center) at the University of Kentucky and the American Institute for Steel Construction through the AISC Fellowship program. Their support is gratefully acknowledged.

REFERENCES

1. Bathe, K.J. (1982), Finite Element Procedures in Engineering Analysis, Prentice-Hall, Inc., Englewood Cliffs, NJ.

2. Bevins, T.L. (1985), Limit Load of Space Truss Structures Composed of Members Subjected to Local and Overall Buckling, thesis presented to the University of Kentucky, at Lexington, KY, in partial fulfillment of the requirements for the degree of Master of Science.

3. Blandford, G.E., Wang, S.T., and Hill, C.D. (1988), "Stability and Post-Buckling Analysis of Steel Space Trusses", Proceedings, Structural Stability Research Council, Minneapolis, Minnesota, April, 1988.

4. Chu, K-H. and Rampetsreiter, R.H. (1972), "Large Deflection Buckling of Space Frames", Journal of the Structural Division, ASCE, Vol. 98, ST12, pp. 2701-2722.

5. Crisfield, M.A. (1983), "An Arc-Length Method Including Line Searches and Accelerations," International Journal for Numerical Methods in Engineering, Vol. 19, pp. 1269 - 1289

6. Jagannathan, D.S., Epstein, H.I. and Christiano, P. (1975), "Nonlinear Analysis of Retriculated Space Trusses", Journal of the Structural Division, ASCE, Vol. 101, No. ST12, pp. 2641-2658.

7. Kondoh, K. and Atluri, S.N. (1985), "Influence of Local Buckling on Global Instability: Simplified, Large Deformation, Post-Buckling Analyses of Plane Trusses", Computers and Structures, Vol. 21, No. 4, pp. 613-627.

8. Lev Zetlin and Associates (1978), Report on the Causes of the Collapse of the Hartford Coliseum Space Truss Roof, Submitted to the City of Hartford, CT.

9. Papadrakakis, M. (1983), "Inelastic Post-Buckling Analysis of Trusses", Journal of the Structural Division, ASCE, Vol. 109, ST9, pp. 2129-2147.

10. Prickett, S.C., and Mueller, W.H., Limit Analysis of Lattice Structures, Structural Analysis Program, Bonneville Power Association, Portland, Oregon, June, 1983.

11. Richard, R.M. and Blacklock, J.R. (1969), "Finite Element Analysis of Inelastic Structures", AIAA Journal, 7(3), 432-438.

12. Rosen, A., and Schmidt, L.A., Jr., "Design Oriented Analysis of Imperfect Truss Structures: Part I - Accurate Analysis", International Journal for Numerical Methods in Engineering, Vol. 14, 1979, pp. 1309-1321.

13. Task Committee on Latticed Structures (1976), "Latticed Structures: State of the Art Report", Journal of the Structural Division, ASCE, Vol. 102, ST11, pp. 2192-2230.

14. Timoshenko, S.P. and Gere, J.M. (1961), Theory of Elastic Stability, McGraw-Hill, New York, NY.

15. Wang, S.T. and Bevins, T. L. (1987), "Stability and Limit Loads of Steel Space Trusses", Materials and Member Behavior, D.S. Ellifritt (Editor), Proceedings of the Structures Congress '87, Orlando, FL, August 17-20, ASCE, New York, NY, pp. 15-29.

16. Wang, S.T., Errera, S.J. and Winter, G. (1975), Behavior of Cold Rolled Stainless Steel Members", Journal of the Structural Division, ASCE, Vol. 101, ST11, pp. 2337-2357.

17. Weaver, W. and Gere, J.M. (1980), Matrix Analysis of Framed Structures, D. Van Nostrand Co., New York, NY.

18. Winter, G. (1968), "Thin-Walled Cold-Formed Steel Structures: Theory and Design", International Association for Bridge and Structural Engineering, Eighth Congress, New York, NY.

Table 1 - Cross section types used for space trusses

Truss	Members	Cross-section Type
T1	ALL	SC1
T2	ALL	I1
T3	1 to 4, 9 to 12	I2
	5 to 8, 13 to 16	I2
	17 to 32	I3
	33 to 36	I2
T4	Top Chords	I2
	Bottom Chords	I2
	Diagonals	I4

Table 2 - Member properties used for space trusses (units shown with elastic modulus)

MEMBER NAME	SECTION TYPE	DIMENSIONS				AREA	ELASTIC MODULUS (E)
		DEPTH (d)	WEB THICKNESS (t_w)	FLANGE WIDTH (b_f)	FLANGE THICKNESS (t_f)		
SC1	SOLID CIRCULAR	N/A	N/A	N/A	N/A	96.77	7.03E+5 kg/cm^2
I1	I-SECTION	4.15	0.15	2.50	0.15	1.3275	3.0E+4 KSI
I2	"	8.075	0.15	4.00	0.075	1.7888	"
I3	"	6.05	0.10	3.00	0.05	0.895	"
I4	"	4.075	0.075	4.00	0.075	1.1888	"

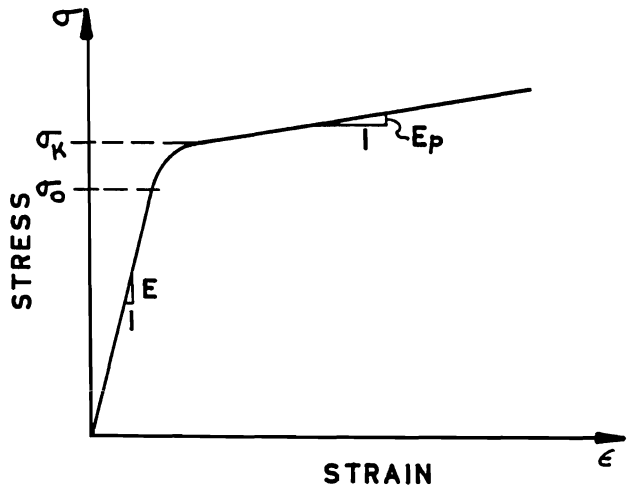

Fig. 1 - Stress-strain behavior modeling
(Richard and Blacklock, 1969)

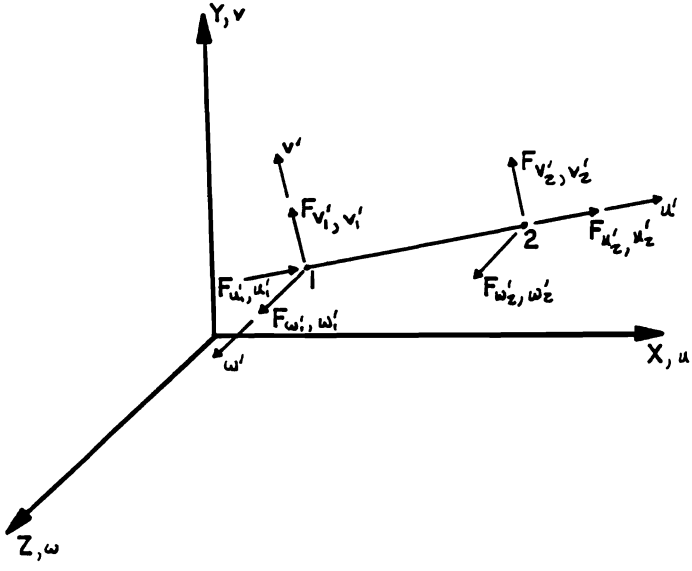

Fig. 2 - Local coordinate forces and displacements
for a space truss element

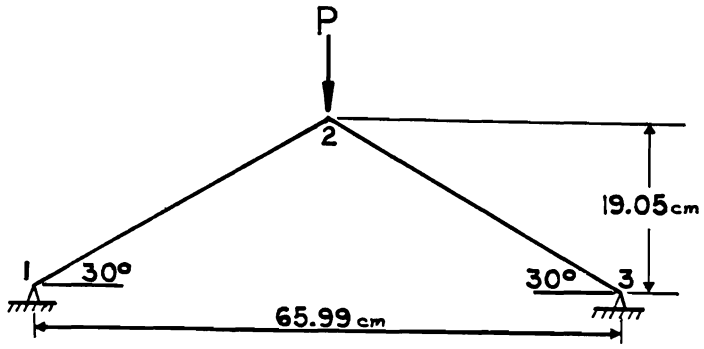

Fig. 3 - Geometry and loading for truss T1

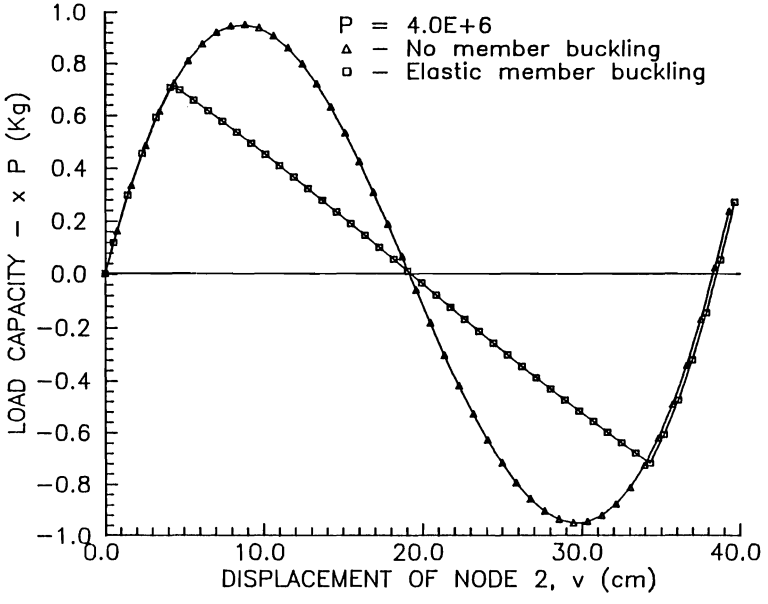

Fig. 4 - Load-displacement curve for truss T1
(displacements at node 2)

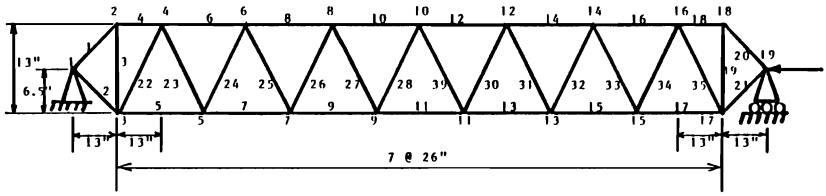

Fig. 5 - Geometry and loading for truss T2

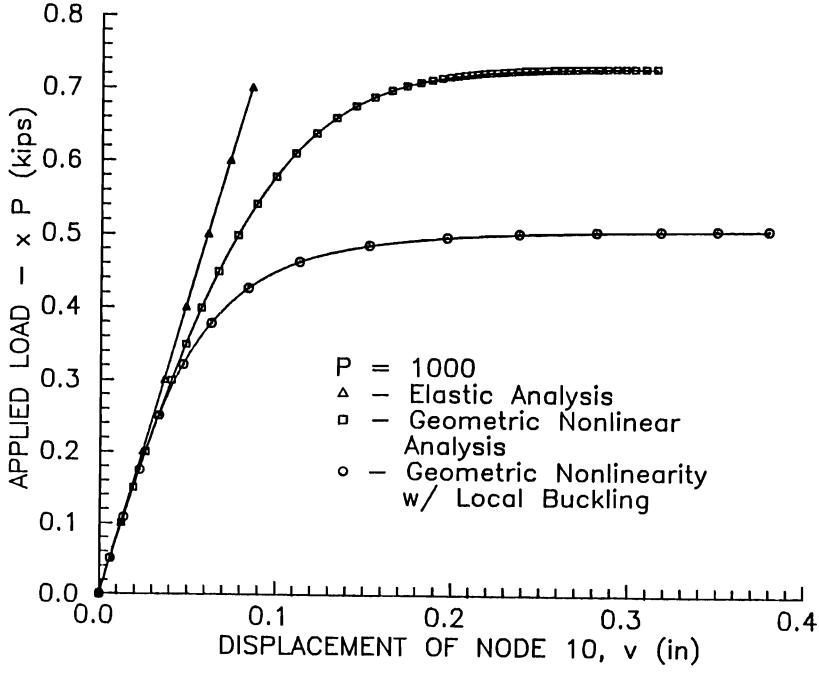

Fig. 6 - Load-dsiplacement curves for truss T2 (displacements at node 10)

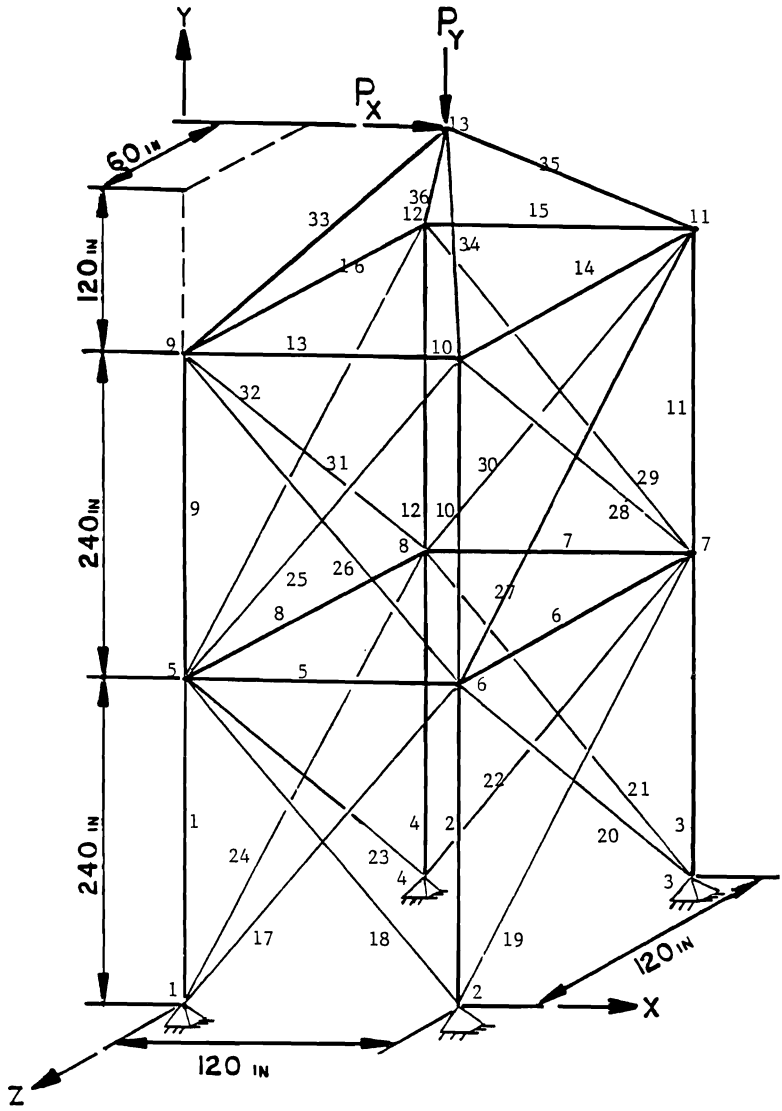

Fig. 7 - Geometry and loading for truss T3

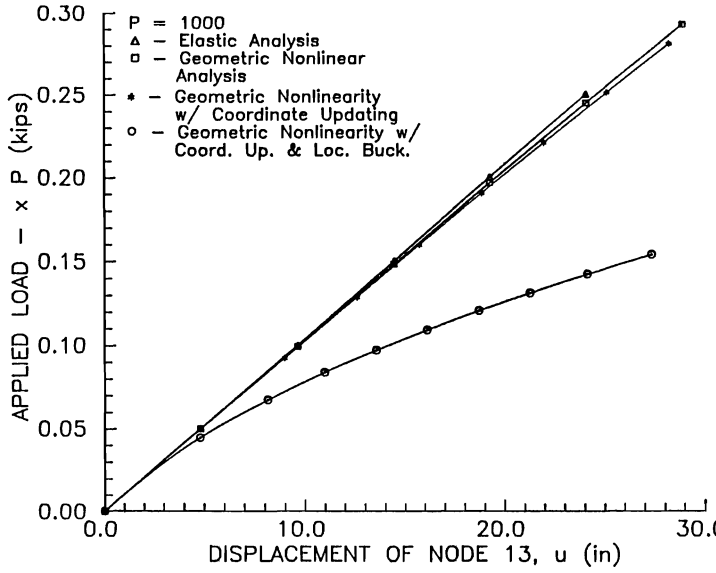

Fig. 8 - Load-displacement curves for truss T3 (displacements at node 13)

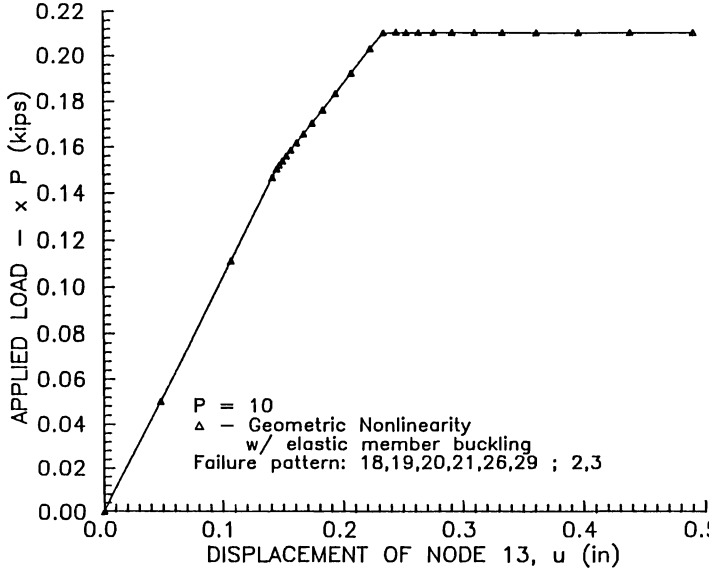

Fig. 9 - Load-displacement curve for truss T3 with member failures (displacements at node 13)

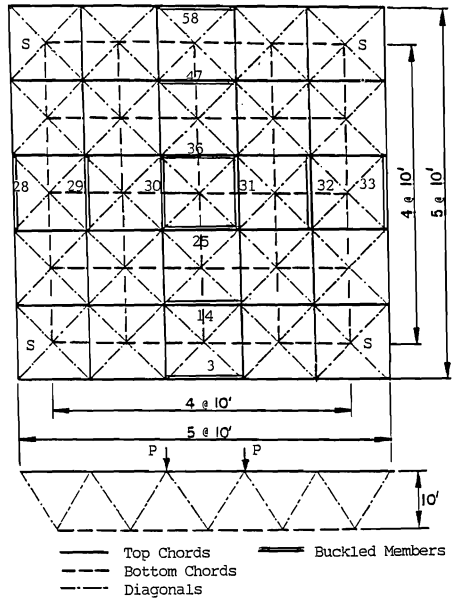

Fig. 10 - Geometry, loading, and member failures for truss T4

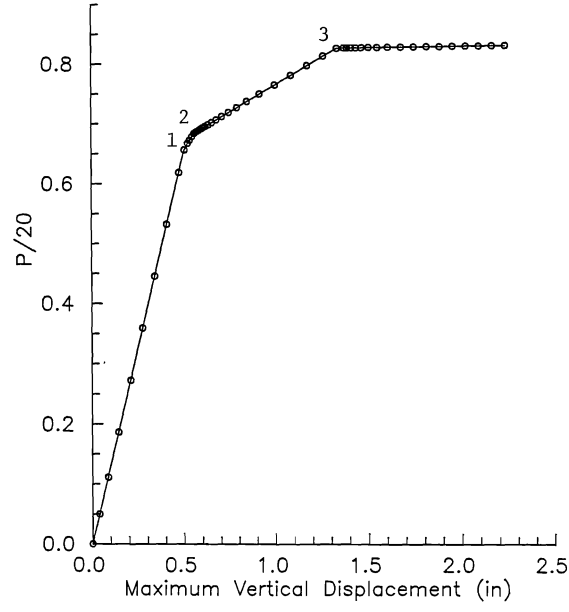

Fig. 11 - Load-displacement curve for truss T4 with member failures